Pak. J. Bot., 59(4): April 2027.

ARTICLE | DOI: http://dx.doi.org/10.30848/PJB2027-4(7)

THE MITOCHONDRIAL GENOME OF *PINUS SYLVESTRIS* VAR. *MONGOLICA* LITV. (PINALES: PINACEAE)

JIAN-HUA LIU*, QING MA, QING-HUI MA AND SEN-YAO LIU

Liaoning Research Institute of Sand Control and Utilization, Liaoning Zhanggutai Desert Ecosystem Research Station, Fuxin 123000, Liaoning, China

*Corresponding author's email: ljh_gudu@163.com

Abstract

We used Illumina and Nanopore data to complete the sequencing and assembly of mitochondrial genome of *Pinus sylvestris* var. *mongolica*, an important coniferous tree species adapted to arid and semi-arid ecosystems. The genome comprises 2,273,603 bp with a GC content of 46.80% (A: 26.56%, T: 26.65%, C: 23.47%, G: 23.33%) and features both molecule 1 and molecule 2 components. It encodes 39 protein-coding, 11 tRNA, and three rRNA genes, with notable gene duplications and intron-rich regions. Phylogenetic analysis places *P. sylvestris* var. *mongolica* within *Pinus*. Under the limited set of publicly available Pinaceae mitogenomes, *Pinus* and *Cathaya* are adjacent in the tree

Key words: Mitochondrial genome; *Pinus sylvestris* var. *mongolica*; Phylogenetic analysis

Introduction

The Mongolian Scots pine, *Pinus sylvestris* var. *mongolica* Litv. (Pinaceae), is an ecologically and economically significant coniferous tree (Fig. 1). It is a geographically distinct variety of Scots pine (*Pinus sylvestris* L.), primarily distributed across the harsh continental climate regions of Mongolia, as well as northern and northeastern China (Wuyuntana *et al.,* 2025).

The tree is characterized by a straight trunk with flaky bark that transitions from greyish-brown at the base to orange-red or copper-brown upwards; twisted needles arranged in pairs; and ovoid to conical cones that mature to a greyish-brown colour. Renowned for its exceptional resilience, *P. sylvestris* var. *mongolica* exhibits remarkable tolerance to drought, low temperatures, and nutrient-poor sandy soils, forming stable forest ecosystems on marginal lands (Zhang *et al.,* 2022).

Plant mitochondrial genomes hold significant value for evolutionary and phylogenetic studies due to their distinctive features, including relatively conserved gene content, low substitution rates, and frequent structural rearrangements (Gualberto *et al.,* 2014). In Pinaceae, mitochondrial genomes are generally maternally inherited, while plastid genomes are paternally inherited (Neale *et al.,* 1989). Therefore, mitochondrial markers provide valuable information for tracking seed-mediated gene flow, making this assembled mitogenome a useful resource for future population genetic and conservation studies of *P. sylvestris* var. *mongolica*. These characteristics make them particularly useful for resolving deep phylogenetic relationships and understanding genomic evolution at higher taxonomic levels (Mower *et al.,* 2012).

Given its ecological and economic value, *P. sylvestris* var. *mongolica* has been a subject of genetic and genomic studies. However, these efforts have primarily utilized chloroplast genome data (Yu *et al.,* 2022) and nuclear markers (Fang *et al.,* 2014), while its mitochondrial (mt) genome remains completely uncharacterized. This gap limits the development of potential mitochondrial DNA markers for population genetics, species identification and conservation of this species (Birky, 2001). To enrich the genomic resources for this ecologically vital tree and contribute to the broader phylogenomic framework of *Pinus*, we sequenced, assembled, and annotated the complete mitochondrial genome of *P. sylvestris* var. *mongolica* using Illumina and Nanopore sequencing data.

Materials and Methods

Sample collection and DNA extraction: Needle samples of *P. sylvestris* var. *mongolica* were collected from a single individual at Zhanggutai Township, Liaoning Province, China (42°22′N, 122°31′E) and deposited at the Liaoning Research Institute of Sand Control and Utilization, under voucher number SEW2230 (contact: Jian-Hua Liu, ljh_gudu@163.com). The collected tree species were identified by morphological examination consistent with the Flora of China (Zheng *et al.,* 1978). Genomic DNA was extracted from needle samples using a modified CTAB method (Murray *et al.,* 1980) and stored at -20°C.

Mitochondrial genome sequencing, assembly, and annotation: Nanopore long-read libraries were constructed using the SQK-LSK109 ligation kit and sequenced on a PromethION platform. Raw Nanopore data (51.5 Gb) were quality filtered with NanoPack from NanoPack suite (De Coster *et al.,* 2018), yielding 49.8 Gb clean data originating from 3.57 million reads with an average read length of 14,008 bp. Illumina paired end libraries with 350 bp insert size were prepared using the NexteraXT DNA Library Preparation Kit and sequenced on the NovaSeq 6000

Received: 18-08-2026 | Revised: 15-10-2026 | Accepted: 20-10-2026 | Online: 05-11-2026

platform. Raw short read data were processed with NGS QC Tool Kit v2.3.3 (Patel *et al.,* 2012), resulting in 106.7 Gb clean data from 355.72 million reads.

For mitochondrial assembly, Nanopore reads were aligned to published Pinaceae mitochondrial reference sequences (*Pinus taeda* NC_039746.1; *Picea sitchensis* MK697696.1; *Abies alba* ON378818.1; *Larix sibirica* MT797187.1) using minimap2 (v2.15-r905) with the parameter "-ax map-ont". Reads producing valid alignments against these references were assembled with Miniasm (v0.3-r179) (Li, 2016) to generate an initial assembly built from long reads, which was then iteratively polished with NextPolish (v1.3.1) (Hu *et al.,* 2020) to correct base errors. Quality filtered Illumina reads were mapped to these polished contigs using bowtie2 (v2.3.5.1) (Langmead *et al.,* 2012), and Unicycler (v0.4.8) (Wick *et al.,* 2017) was applied for assembly of mapped Illumina reads, generating additional contig sequences using only short-read information. All contigs were imported into Bandage (v0.8.1) (Wick *et al.,* 2015) for assembly graph visualization. Nanopore reads were re-aligned to the full contig set via minimap2 (Li, 2018), and contig connections were confirmed by integrating Bandage graph topology and alignment evidence from long reads.

Mitochondrial contigs were separated from chloroplast derived contigs and nuclear NUMT contigs after assembly, based on distinct read coverage levels and graph topology in Bandage. Edges within the assembly graph are supported by Nanopore read coverage and spanning reads across repeat junctions. The predominant path of molecule 1 was manually selected from the graph topology, informed by both spanning read support and long-read coverage patterns at contig boundaries. Contig connections were validated by long-read coverage at contig boundaries, and no spanning Nanopore reads link molecule 2 to molecule 1. The read counts supporting alternative repeat mediated arrangements at variable junctions are provided in supplementary Table S1.

Genome annotation was performed in parallel using MITOFY (Alverson *et al*., 2010) and PMGA (Li *et al*., 2025) (Plant Mitochondrial Genome Annotator). PMGA integrates tRNAscan-SE (Lowe *et al.*, 2016) for tRNA prediction and adopts plant mitochondrial rRNA reference datasets, while MITOFY identifies homologous tRNA and rRNA regions via BLASTn (Chen *et al*., 2015) searches. Gene predictions from the two tools were cross compared, and all gene boundaries were manually inspected and curated. tRNAs with full-length high-identity matches to chloroplast homologs were annotated as putative chloroplast-derived tRNAs. Specifically, *trnT-GGT* and *trnW-CCA* exhibited 100% sequence identity to chloroplast-encoded tRNAs. Final mitogenome sequences were visualized with OGDRAW (v1.3.1) (Greiner *et al.,* 2019) and submitted to GenBank under accession numbers PX135030.1-PX135031.1.

Phylogenetic analysis: Gymnosperm mitochondrial genome sequences were downloaded from GenBank, including seven Pinaceae species (*Abies beshanzuensis*, *Abies koreana*, *Abies sachalinensis*, *Cathaya argyrophylla*, *Larix sibirica*, *Pinus taeda* and *Pinus tabuliformis*) and two outgroup species (*Ginkgo biloba* and *Cycas taitungensis*). The 35 shared PCGs were aligned with MAFFT v7.037 (Katoh *et al.,* 2013). We inferred the maximum-likelihood phylogeny in IQ-TREE v2.2.0 (Nguyen *et al.,* 2014) conducting 10,000 ultrafast bootstrap replicates to evaluate branch support. The best-fit substitution model was selected using ModelFinder (Kalyaanamoorthy *et al.,* 2017) under the Bayesian information criterion (BIC), yielding TIM+F+G4. The evolutionary tree was visualized with ITOL v6.0 (Letunic *et al.,* 2024).



Fig. 1. Photographs of *Pinus sylvestris* var. *mongolica*.
Note: A: Mature trees, B: Needles and cones.

Results

Characteristics of mitochondrial genome: The complete mitochondrial genome of *P. sylvestris* var. *mongolica* contained 16 contigs, ranging in length from 11,407 to 536,175 bp (Fig. S1). For subsequent analysis, we assembled the contigs into two molecules (Fig. S2). The complete mitochondrial genome of *P. sylvestris* var. *mongolica* has a total length of 2,273,603 bp, comprising a molecule 1 of 2,201,414 bp and a molecule 2 of 72,189 bp (Fig. 2). The overall GC content is 46.80%, and the base composition is 26.56% A, 26.65% T, 23.47% C, and 23.33% G. Coverage of the assembled contigs by both Illumina and Nanopore reads is shown in Fig. S3.

The mitochondrial genome of *P. sylvestris* var. *mongolica* contains 39 PCGs, 11 tRNA genes and three rRNA genes. The PCGs consist of five ATP synthase genes (*atp1*, *atp4*, *atp6*, *atp8*, *atp9*), four cytochrome c biogenesis genes (*ccmB*, *ccmC*, *ccmFc*, *ccmFn*), one ubiquinol cytochrome c reductase gene (*cob*), three cytochrome c oxidase genes (*cox1-3*), one maturase gene (*matR*), one transport membrane protein gene (*mttB*), nine NADH dehydrogenase genes (*nad1-7*, *nad4L*, *nad9*), 13 ribosomal protein genes (*rpl5*, *rpl10*, *rpl16*, *rps1-4*, *rps7*, *rps11-14*, *rps19*), and two succinate dehydrogenase genes (*sdh3* and *sdh4*). Multiple copies of several genes were identified. Among PCGs, *ccmB* and *sdh*3 have two copies The apparent multiple occurrences of *cox1* and *nad4L* along the linearized path are an artefact caused by repeated traversal of repeat contigs and do not represent independent copies. For rRNA genes, *rrn18* has three copies, *rrn5* has three copies. Among tRNA genes, *trnD-GTC* and *trnH-GTG* have two copies each, *trnP-TGG* has three copies, *trnW-CCA* has four copies, and *trnM-CAT* has seven copies. The repeat contigs (contigs 12, 13, 14 and 15) contain gene *cox1*, *sdh3*, *nad4L*, *rrn5*, *rrn26*, *trnW-CCA* and *trnM-CAT*. The apparent multiple occurrences of these genes along the linearized path are artifacts caused by repeated traversal of overlapping populations and are not counted as independent copies. Furthermore, six genes are trans-spliced (*nad1*, *nad2*, *nad4*, *nad5*, *nad7*, and *cox2*) (Fig. 3), and three genes are cis-spliced (*ccmFc*, *rps1*, and *rps3*) (Fig. 4).

Phylogenetic analysis: We constructed a phylogenetic tree using mitochondrial genome sequences from seven Pinaceae species. *Ginkgo biloba* and *Cycas taitungensis* were included as outgroups in the analysis. The results showed that *P. sylvestris* var. *mongolica* clusters with the other two *Pinus* species with 100% bootstrap support. Among the four Pinaceae genera included, *Pinus* and *Cathaya* appear adjacent in the ML tree. (Fig. 5).

The 35 shared PCGs were included in the phylogenetic analysis:*atp1*, *atp4*, *atp6*, *atp8*, *atp9*, *ccmB*, *ccmC*, *ccmFc*, *ccmFn*, *cob*, *cox1-3*, *matR*, *mttB*, *nad1-4*, *nad4L*, *nad5-7*, *nad9*, *rpl5*, *rps1-4*, *rps7*, *rps11-13*, *rps19*, and *sdh3*. The mitochondrial genome sequences involved include: *Abies beshanzuensis* PV744515.1->PV744524.1 (Liu *et al.,* 2025), *Abies koreana* NC_071216.1 (Park *et al.,* 2024), *Abies sachalinensis* PQ275616.1->PQ275627.1 (unpublished), *Cathaya argyrophylla* PP764533.1->PP764541.1 (Huang *et al.,* 2025), *Larix sibirica* MT797187.1->MT797195.1 (Putintseva *et al.,* 2020), *Pinus sylvestris* var. *mongolica* PX135030.1->PX135031.1 (this study), *Pinus taeda* NC_039746.1 (unpublished), *Pinus tabuliformis* PQ399694.1->PQ399695.1 (unpublished), *Ginkgo biloba* NC_027976 (Guo *et al.,* 2016), and *Cycas taitungensis* NC_010303.1 (Chaw *et al.,* 2008).

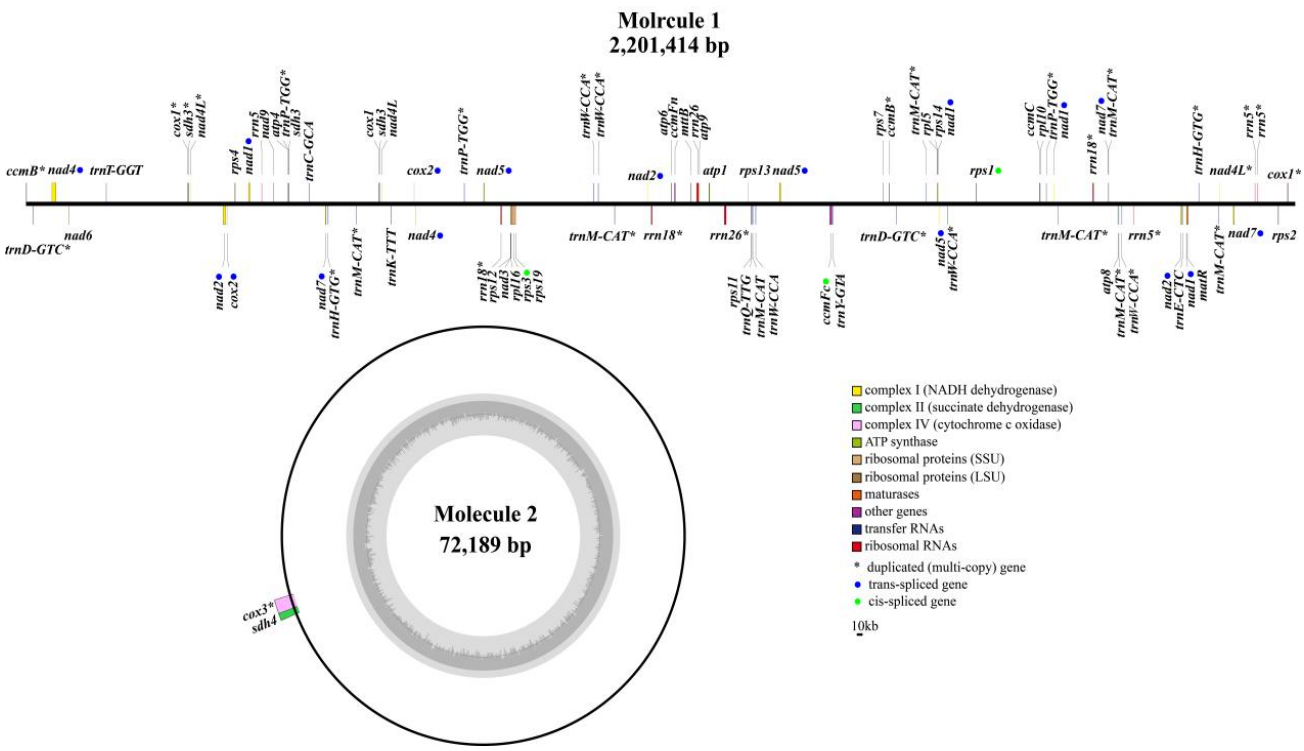


Fig. 2. Map of the mitochondrial genome of *P. sylvestris* var. *mongolica*. Genes located on the inner side of the circle are transcribed in the counterclockwise direction, while those on the outer side are transcribed clockwise. Genes are color-coded according to their functional categories.

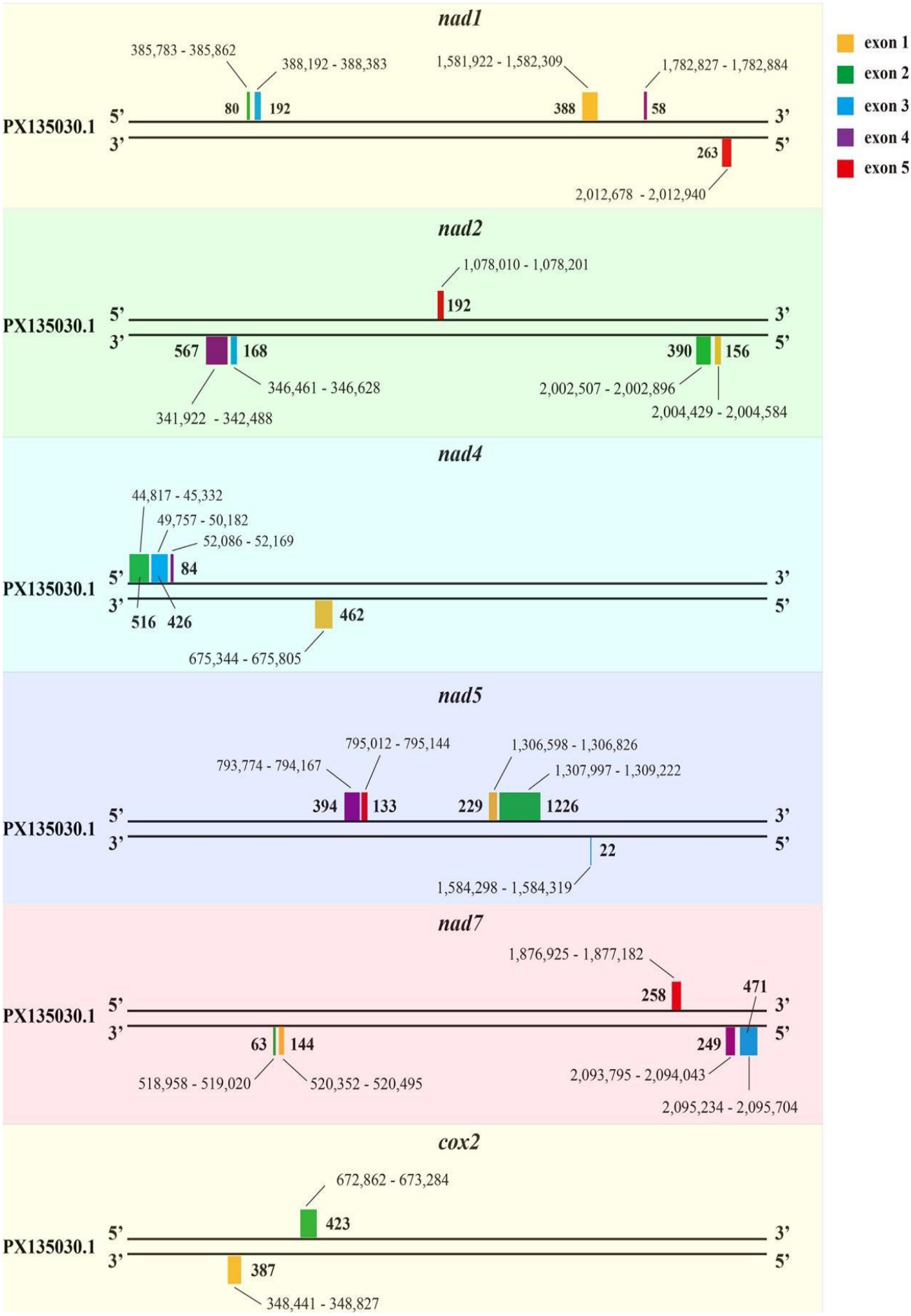


Fig. 3. The trans-splicing gene structure map.

Table S1. Nanopore spanning read counts for repeat-mediated alternative configurations in the mitochondrial assembly graph of *P. sylvestris* var. *mongolica*.

Path ID	Middle node	Middle length bp	Path	Reverse complement path	Support reads
1.	12	21326	2- -> 12+ -> 1+	1- -> 12- -> 2+	2
2.	12	21326	2- -> 12+ -> 8+	8- -> 12- -> 2+	1
3.	12	21326	6+ -> 12+ -> 1+	1- -> 12- -> 6-	3
4.	12	21326	6+ -> 12+ -> 8+	8- -> 12- -> 6-	3
5.	13	16929	1+ -> 13+ -> 11+	11- -> 13- -> 1-	14
6.	13	16929	1+ -> 13+ -> 11-	11+ -> 13- -> 1-	15
7.	13	16929	10- -> 13+ -> 11+	11- -> 13- -> 10+	10
8.	13	16929	10- -> 13+ -> 11-	11+ -> 13- -> 10+	9
9.	14	14812	6- -> 14+ -> 5+	5- -> 14- -> 6+	8
10.	14	14812	6- -> 14+ -> 8-	8+ -> 14- -> 6+	4
11.	14	14812	9+ -> 14+ -> 5+	5- -> 14- -> 9-	9
12.	14	14812	9+ -> 14+ -> 8-	8+ -> 14- -> 9-	7
13.	15	11407	3- -> 15+ -> 10-	10+ -> 15- -> 3+	8
14.	15	11407	3- -> 15+ -> 4-	4+ -> 15- -> 3+	8
15.	15	11407	5+ -> 15+ -> 10-	10+ -> 15- -> 5-	9
16.	15	11407	5+ -> 15+ -> 4-	4+ -> 15- -> 5-	14

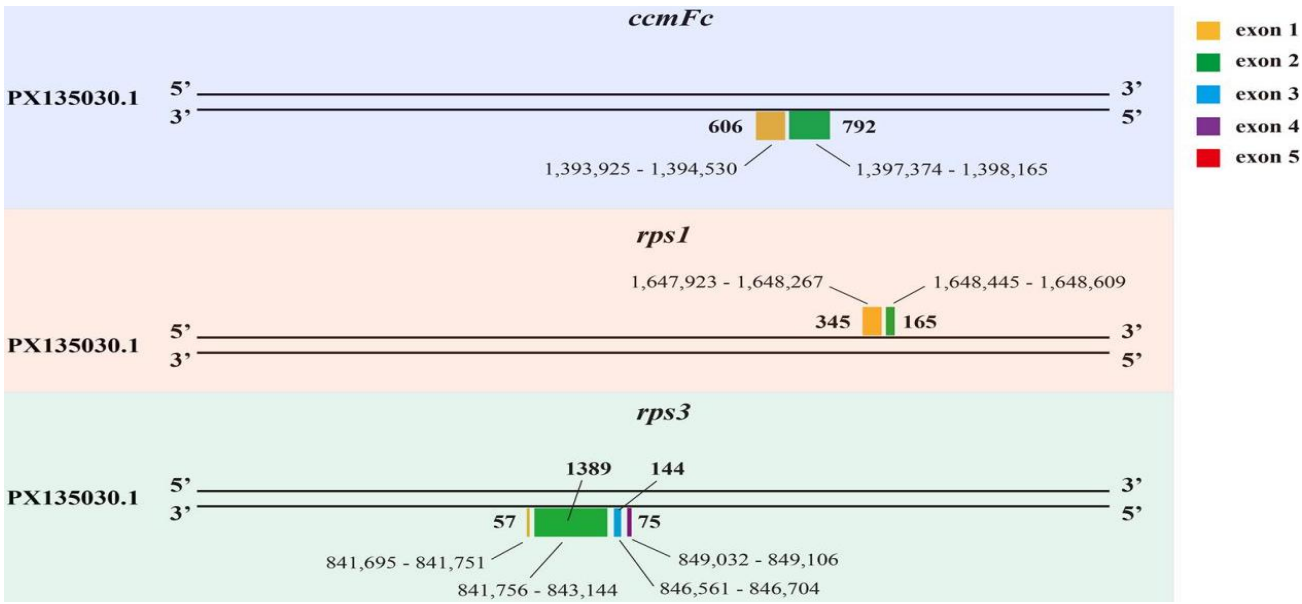


Fig. 4. The cis-splicing gene structure maps.

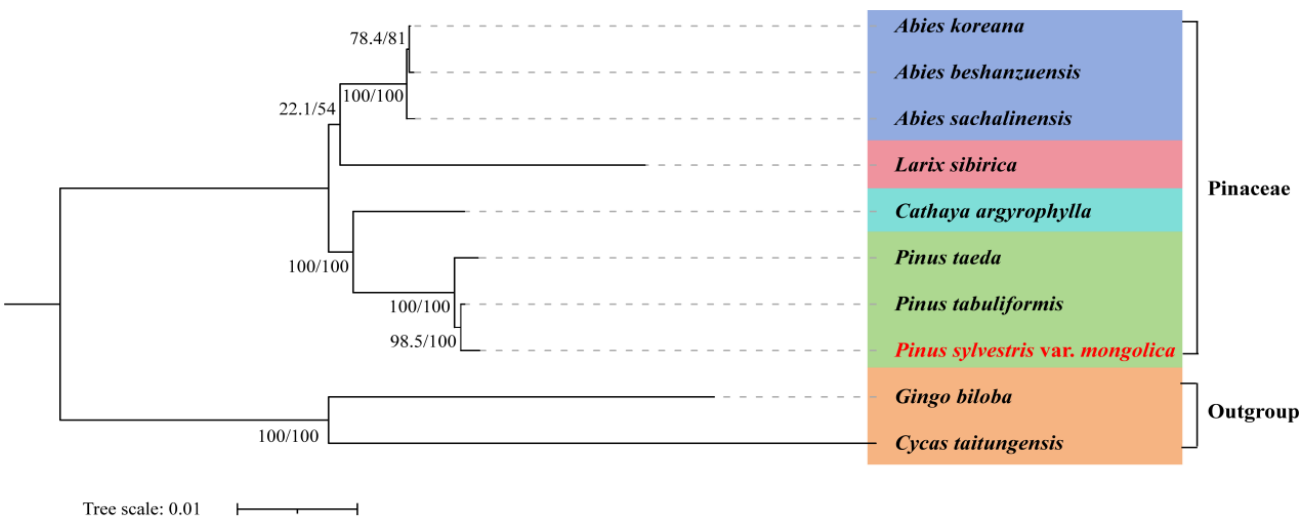


Fig. 5. A maximum-likelihood phylogenetic tree constructed from 10 mitochondrial genomes. Numbers on the branches are SH-aLRT/UFBoot2 support values. Nodes with SH-aLRT≥80 and UFBoot2≥95 are considered strongly supported.

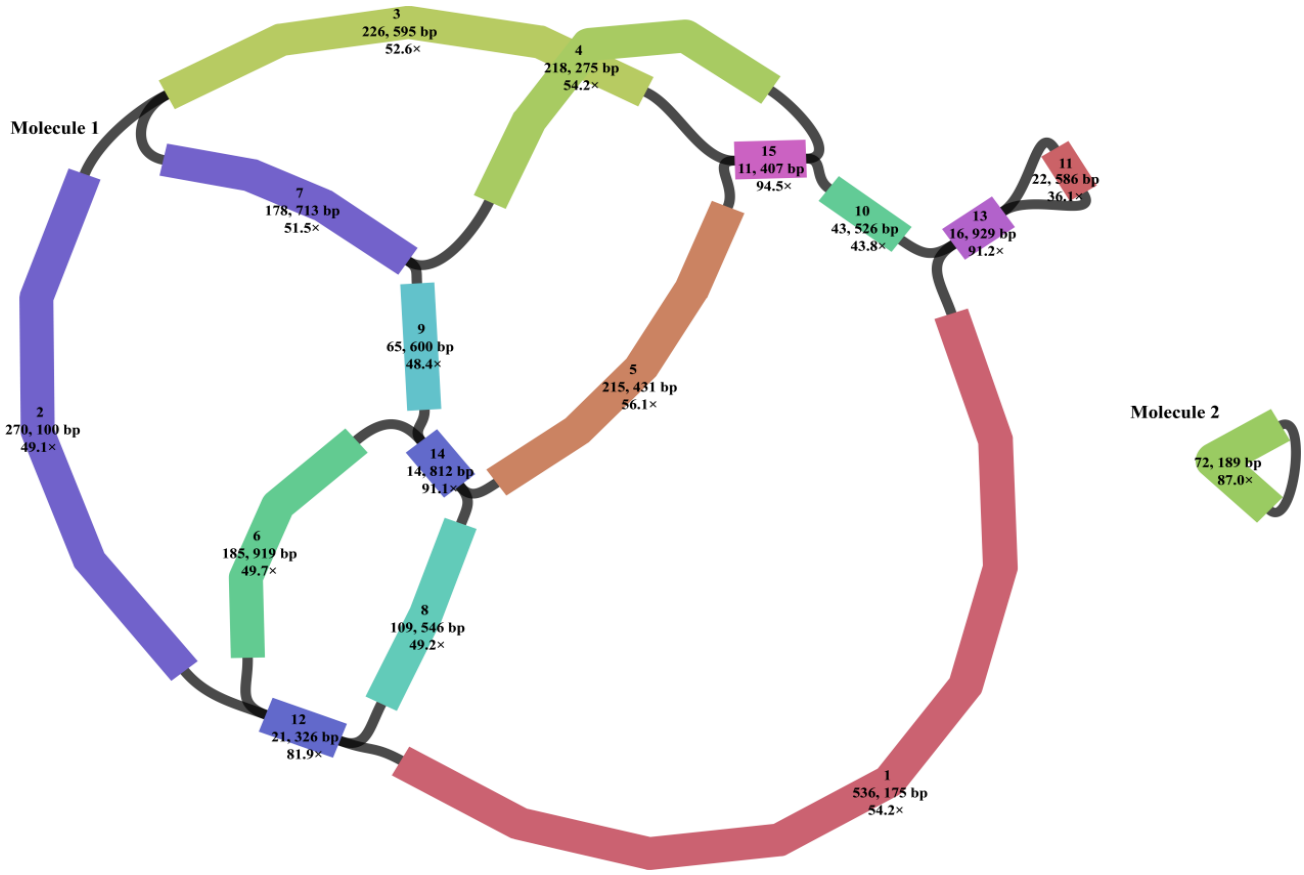


Fig. S1. Assembly results of the mitochondrial genome of *Pinus sylvestris* var. *mongolica*. The numbers on the line represent the order in which each contig was arranged from largest to smallest, as well as the size of each contig.

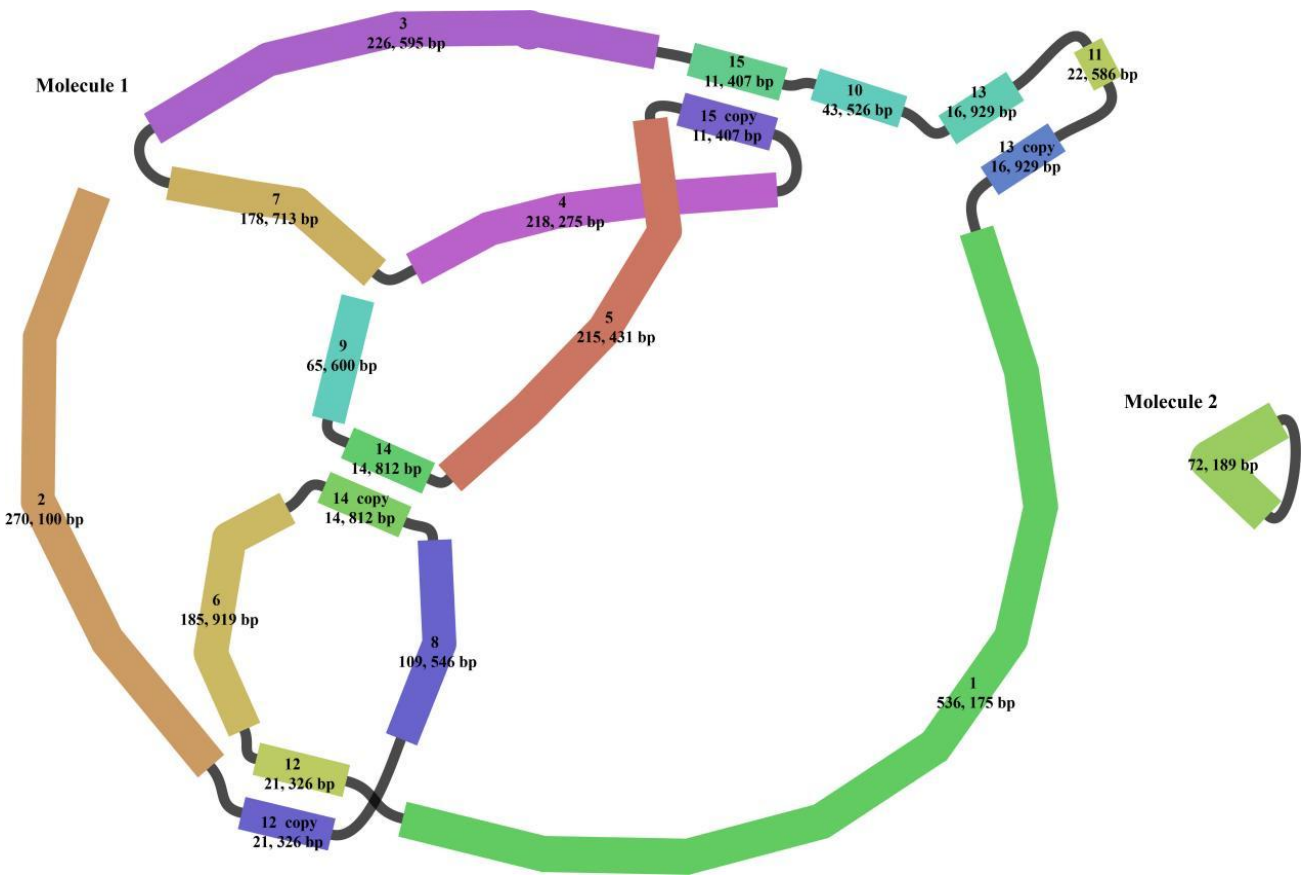


Fig. S2. The structure of mitochondrial genome of *Pinus sylvestris* var. *mongolica* after linearization. The arrangement order of contigs in molecule 1: 2-12 copy-8-14 copy-6-12-1-13 copy-11-13-10-15-3-7-4-15 copy-5-14-9.

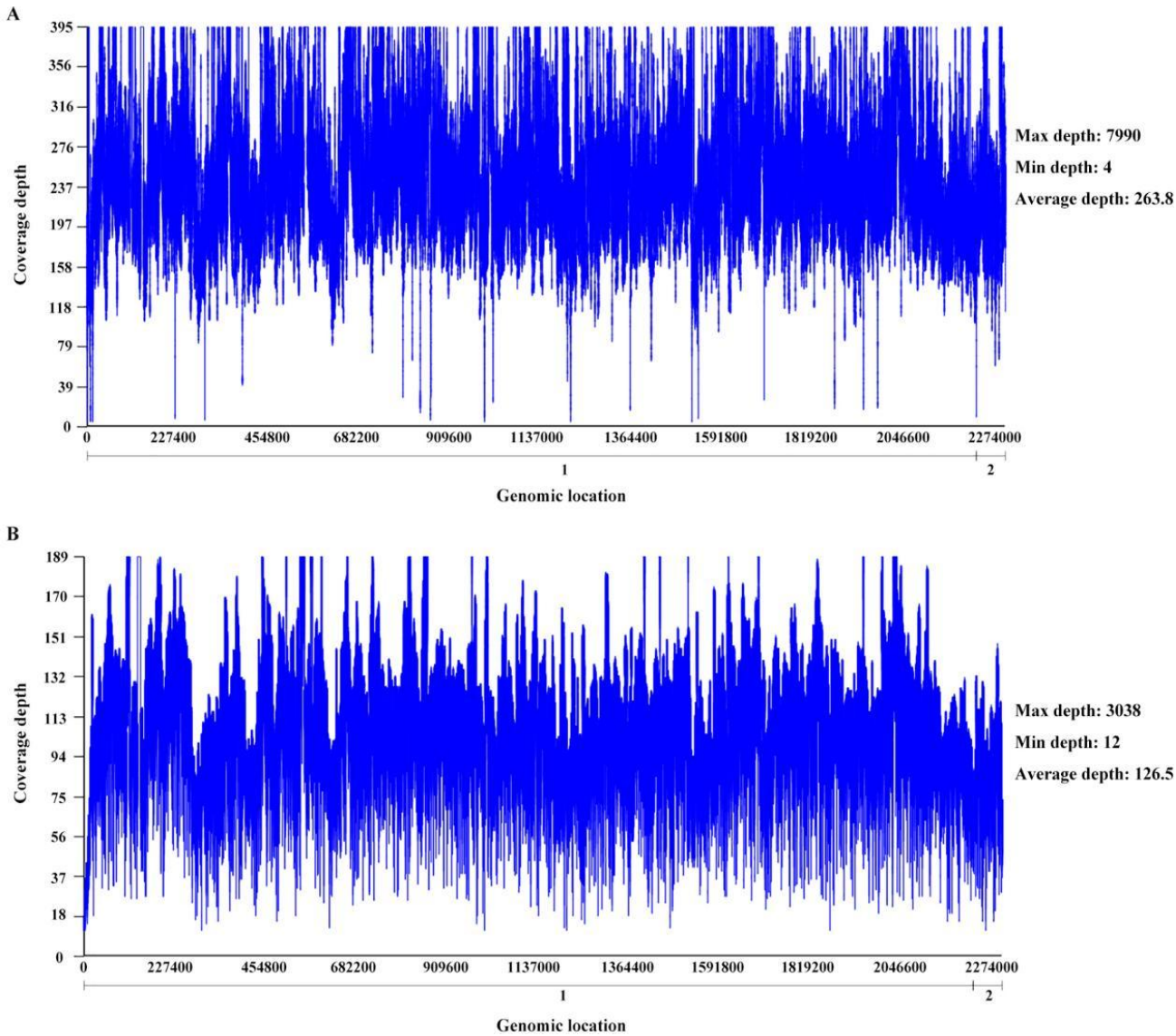


Fig. S3. A: The coverage-depth map of Illumina sequencing, B: The coverage-depth map of Nanopore sequencing.

Discussion

Structural characteristics of the *P. sylvestris* var. *Mongolica* mitogenome: This study presents the complete mitochondrial genome assembly of *P. sylvestris* var. *mongolica*, which exhibits a massive genome size of 2,273,603 bp and a complex multi-partite architecture containing two molecules, consistent with the widely reported mitochondrial features observed across Pinaceae gymnosperms (Putintseva *et al.,* 2020; Huang *et al.,* 2025). Compared with the Pinaceae mitogenomes, the 2.27 Mb mitogenome of *P. sylvestris* var. *mongolica* falls between the small *P. taeda* (1.19 Mb) and the large genomes of *L. sibirica* (11.66 Mb), and *C. argyrophylla* (18.99 Mb). A shared feature across these Pinaceae mitogenomes is a complex, branched, multipartite organization in which repetitive sequences mediate homologous recombination and generate multiple alternative isoforms; this is consistent with the multi-contig structures reported in *L. sibirica* (nine contigs) and *C. argyrophylla* (six linear and three circular contigs) (Putintseva *et al.,* 2020; Huang *et al.,* 2025). Abundant gene duplications and numerous intron-harbouring loci, including six trans-spliced and three cis-spliced genes, were detected within this mitogenome. In terms of gene duplication, the present mitogenome contains multi-copy genes, including two copies of *ccmB* and *sdh3*, and multiple copies of rRNA and tRNA genes (e.g., *rrn5* in three copies and *trnM-CAT* in seven copies). Such gene copy-number variation has been repeatedly reported across Pinaceae mitogenomes and is commonly associated with repeat-mediated duplication and rearrangement rather than with functional divergence (Gualberto *et al.,* 2014; Mower *et al.,* 2012). These duplicated copies are most likely recombination-mediated by-products rather than functional paralogs, and mark the elevated recombination activity of Pinaceae mitogenomes.

Six genes (*nad1*, *nad2*, *nad4*, *nad5*, *nad7*, *cox2*) are trans-spliced and three (*ccmFc*, *rps1*, *rps3*) are cis-spliced in the present genome. A high proportion of trans-spliced introns, together with conserved cis-spliced loci, is a conserved feature of Pinaceae (and other gymnosperm) mitogenomes, in which widespread genomic rearrangement and recombination disperse exons and require trans-spliced maturation (Guo *et al.,* 2020). These intron-rich loci carry mostly group II introns, and the cis-to-trans dispersal of their exons reflects the mitogenome's

extensive rearrangement history; trans-splicing is required to reassemble mature mRNAs, and intron gains/losses or splicing shifts additionally serve as phylogenetically informative evolutionary markers (Guo *et al.,* 2020). Overall, the repeated gene copies and dispersed, trans-spliced introns observed here align with the recombination-driven structural complexity that characterizes Pinaceae mitogenomes rather than representing lineage-specific gains or losses.

Phylogenetic relationships within Pinaceae inferred from mitochondrial PCGs: Our maximum-likelihood phylogeny built from 35 conserved mitochondrial protein-coding genes yielded robust topological support. In our limited sampling, *Pinus* and *Cathaya* were recovered adjacent in the mitochondrial tree. However, because few complete Pinaceae mitogenomes were publicly available at the time of analysis, this topology does not constitute confirmed evidence on deep intergeneric relationships, and broader taxon sampling is required (Huang *et al.,* 2025). Notably, *Larix* was recovered together with *Abies* in our mitochondrial phylogeny, a topology inconsistent with the established the pinoid (Pinoideae) and abietoid (Abietoideae) lineages classification of Pinaceae. This grouping received only weak nodal support. This conflicting placement is interpreted as an artifact arising from restricted taxon sampling and the limited number of parsimony-informative sites in the conserved mitochondrial protein-coding dataset. Mitochondrial loci alone may have insufficient phylogenetic signal to fully resolve deep intergeneric relationships in Pinaceae. Broader taxon sampling combined with more informative nuclear loci will be required to resolve these relationships reliably. Prior genetic investigations of *P. sylvestris* var. *mongolica* largely depended on chloroplast sequences and nuclear molecular markers (Yu *et al.,* 2022; Fang *et al.,* 2014). The mitogenome reported here fills this critical data gap for this drought-tolerant sand-fixing conifer.

Genomic resource value and limitations of this study: This assembled mitogenome constitutes a fundamental genomic resource for downstream population genetic surveys, molecular species authentication, and conservation genomic work for *P. sylvestris* var. *mongolica*. It also facilitates cross-conifer comparative studies targeting mitochondrial structural rearrangement and heterogeneous molecular evolutionary rates. Nevertheless, taxon sampling in the present phylogenetic analysis remains limited; only a subset of Pinaceae genera and a small number of *Pinus* representatives were included. Therefore, future research should integrate additional mitochondrial genome datasets from diverse pine species and varieties. Expanded taxon coverage will improve phylogenetic resolution and enable thorough exploration of intrageneric evolutionary dynamics within *Pinus*. Beyond expanding taxon sampling, this reference mitogenome can support population-level surveys of mitochondrial variation, including haplotype and structural polymorphism among natural populations, and the development of mitochondrial markers for conservation genetics, molecular authentication, and phylogeography of this drought-tolerant conifer.

Conclusion

In this research, we obtained and annotated the complete mitochondrial genome of *P. sylvestris* var. *mongolica* using combined Illumina short-read and Nanopore long-read sequencing technology. The mitogenome displays a multi-partite structure with extensive gene duplications and multiple spliced intron-containing genes, reflecting the complex evolutionary characteristics of Pinaceae mitochondrial genomes. Based on 35 shared mitochondrial PCGs, the sampled *Pinus* species form a clade; the adjacency of *Pinus* and *Cathaya* was reported descriptively under restricted taxon sampling.. This work supplies previously-absent mitochondrial genomic data for *P. sylvestris* var. *mongolica*, supporting future conservation, population genetics, and comparative mitogenomic analyses. Owing to restricted taxonomic sampling, further mitogenome sequencing of more pine taxa is required to better decipher the evolutionary history of the genus *Pinus*.

Ethics Statement: The sampling site is located outside of any protected area, and ethical approval is not necessary.

Acknowledgements

We gratefully acknowledge the Liaoning Research Institute of Sand Control and Utilization for its financial and infrastructural support. We thank Professor Wei Li (Beijing Forestry University) for his invaluable guidance on experimental design and technical support. We also appreciate the diligent work of Qi-Jing Xia in conducting experiments and collecting data.

Data Availability Statement: The mitogenome sequence data that support the findings of this study are openly available in GenBank of NCBI at https://www.ncbi.nlm.nih.gov/ under the accession number PX135030.1 and PX135031.1. The associated BioProject, BioSample, and SRA numbers are PRJNA1390325, SAMN54180862, and SRR36495697 (third-generation) and SRR36495696 (second-generation), respectively.

Funding: This work was funded by the research project Technology for Precision Improvement of Shelter Forest Quality on the Southern Edge of the Khorchin Sandy Land under the Agricultural Green and High-Quality Development Plan (No. 2025HQ1311).

Conflict of Interests: The authors declare that they have no known competing financial interests or personal relationships that could have appeared to influence the work reported in this paper.

Author's Contribution: Jian-Hua Liu designed the research and revised the manuscript. Qing Ma performed the bioinformatic analyses and prepared the figures. Qing-Hui Ma assisted with genomic assembly and validation. Sen-Yao Liu collected and identified the sample. All authors read and approved the final manuscript.

References

Alverson, A.J., X. Wei, D.W. Rice, D.B. Stern, K. Barry and J.D. Palmer. 2010. Insights into the evolution of mitochondrial genome size from complete sequences of *Citrullus lanatus* and *Cucurbita pepo* (Cucurbitaceae). *Mol. Biol. Evol*., 27: 1436-1448.

Birky, C.W. Jr. 2001. The inheritance of genes in mitochondria and chloroplasts: laws, mechanisms, and models. *Ann. Rev. Genet.*, 35: 125-148.

Chaw, S.M., A.C. Shih, D. Wang, Y.W. Wu, S.M. Liu and T.Y. Chou. 2008. The mitochondrial genome of the gymnosperm *Cycas taitungensis* contains a novel family of short interspersed elements, Bpu sequences, and abundant RNA editing sites. *Mol. Biol. Evol.*, 25(3): 603-615.

Chen, Y., W. Ye, Y. Zhang and Y. Xu. 2015. High speed BLASTN: an accelerated MegaBLAST search tool. *Nucleic Acids Res.*, 43(16): 7762-7768.

De Coster, W., S. D'Hert, D.T. Schultz, M. Cruts and C. Van Broeckhoven. 2018. NanoPack: Visualizing and processing long-read sequencing data. *Bioinformatics*, 34: 2666-2669.

Fang, P., S. Niu, H. Yuan, Z. Li, Y. Zhang, L. Yuan and W. Li. 2014. Development and characterization of 25 EST-SSR markers in *Pinus sylvestris* var. *Mongolica* (Pinaceae). *Appl. Plant Sci.*, 2(1): 1300057.

Greiner, S., P. Lehwark and R. Bock. 2019. Organellar Genome DRAW (OGDRAW) version 1.3.1: expanded toolkit for the graphical visualization of organellar genomes. *Nucleic Acids Res.*, 47(W1): W59-W64.

Gualberto, J.M., D. Mileshina, C. Wallet, A.K. Niazi, F. Weber-Lotfi and A. Dietrich. 2014. The plant mitochondrial genome: Dynamics and maintenance. *Biochimie*, 100: 107-120.

Guo, W., A. Zhu, W. Fan, R.P. Adams and J.P. Mower. 2020. Extensive shifts from cis- to trans-splicing of gymnosperm mitochondrial introns, *Mol. Biol. Evol.*, 37(6): 1615-1620.

Guo, W., F. Grewe, W. Fan, J.Y. Gregory, K. Volker, D.P. Jeffrey and P.M. Jeffrey. 2016. *Ginkgo* and *Welwitschia* mitogenomes reveal extreme contrasts in gymnosperm mitochondrial evolution. *Mol. Biol. Evol.*, 33(6): 1448-1460.

Hu, J., J. Fan, Z. Sun and S. Liu. 2020. NextPolish: a fast and efficient genome polishing tool for long-read assembly. *Bioinformatics*, 36(7): 2253-2255.

Huang, K., W. Xu, H. Hu, X. Jiang, L. Sun, W. Zhao, B. Long, S. Fan, Z. Zhou, P. Mo, X. Jiang, J. Tian, A. Deng, P. Xie and Y. Wang. 2025. Super-large record-breaking mitochondrial genome of *Cathaya argyrophylla* in Pinaceae. *Front. Plant Sci.*, 16: 1556332.

Kalyaanamoorthy, S., B.Q. Minh, T.K.F Wong, A. von Haeseler and L.S. Jermiin. 2017. ModelFinder: Fast model selection for accurate phylogenetic estimates. *Nat. Methods*, 14: 587-589.

Katoh, K. and D.M. Standley. 2013. MAFFT multiple sequence alignment software version 7: improvements in performance and usability. *Mol. Biol. Evol.*, 30(4): 772-780.

Langmead, B. and S.L. Salzberg. 2012. Fast gapped-read alignment with bowtie 2. *Nat. Methods*, 9(4) :357-359.

Letunic, I. and P. Bork. 2024. Interactive Tree of Life (iTOL) v6: recent updates to the phylogenetic tree display and annotation tool. *Nucleic Acids Res.*, 52(W1): W78-W82.

Li, H. 2016. Minimap and miniasm: fast mapping and de novo assembly for noisy long sequences. *Bioinformatics*, 32(14): 2103-2110.

Li, H. 2018. Minimap2: pairwise alignment for nucleotide sequences. *Bioinformatics*, 34(18): 3094-3100.

Li, J., Y. Ni, Q. Lu, H. Chen and C. Liu. 2025. PMGA: A plant mitochondrial genome annotator. *Plant Commun.*, 6(3): 101191.

Liu, X., S. Hu, J. Shen and M. Li. 2025. Assembly and comparative analysis of the complete mitochondrial genome of *Abies beshanzuensis*: insights into conservation genomics of a critically endangered fir. *BMC Plant Biol.,* 25(1): 1049.

Lowe, T.M. and P.P. Chan. 2016. tRNAscan-SE On-line: integrating search and context for analysis of transfer RNA genes. *Nucleic Acids Res*., 44(W1): W54-W57.

Mower, J.P., D.B. Sloan and A.J. Alverson. 2012. Plant mitochondrial genome diversity: The Genomics revolution. Plant genome diversity Volume 1. Vienna: Springer. 123-144.

Murray, M.G. and W.F. Thompson. 1980. Rapid isolation of high molecular weight plant DNA. *Nucleic Acids Res.*, 8(19): 4321-4325.

Neale, D.B. and R.R. Sederoff. 1989. Paternal inheritance of chloroplast DNA and maternal inheritance of mitochondrial DNA in loblolly pine. *Theor. Appl. Genet.*, 77(2): 212-216.

Nguyen, L.T., H.A. Schmidt, A. von Haeseler and B.Q. Minh. 2014. IQ-TREE: a fast and effective stochastic algorithm for estimating maximum-likelihood phylogenies. *Mol. Biol. Evol.*, 32(1): 268-274.

Park, S., M. Kwak and S. Park. 2024. Complete organelle genomes of Korean fir, *Abies koreana* and phylogenomics of the gymnosperm genus Abies using nuclear and cytoplasmic DNA sequence data. *Sci. Rep.*, 14: 7636.

Patel, R.K. and M. Jain. 2012. NGS QC Toolkit: a toolkit for quality control of next generation sequencing data. *PLoS One*, 07: e30619.

Putintseva, Y.A., E.I. Bondar, E.P. Simonov, V.V. Sharov, N.V. Oreshkova, D.A. Kuzmin, Y.M. Konstantinov, V.N. Shmakov, V.I. Belkov, M.G. Sadovsky, O. Keech and K.V. Krutovsky. 2020. Siberian larch (*Larix sibirica* Ledeb.) mitochondrial genome assembled using both short and long nucleotide sequence reads is currently the largest known mitogenome. *BMC Genom.*, 21: 654.

Wick, R.R., L.M. Judd, C.L. Gorrie and K.E. Holt. 2017. Unicycler: Resolving bacterial genome assemblies from short and long sequencing reads. *PLoS Comp*., *Biol.*, 13(6): e1005595.

Wick, R.R., M.B. Schultz, J. Zobel and K.E. Holt. 2015. Bandage: Interactive visualization of de novo genome assemblies. *Bioinformatics*, 31(20): 3350-3352.

Wuyuntana, Q. Fong, C.Y. Ke, D.M. Gao, M.X. Luo, Y.Z. Yang, R.H. Gao and P. C. Liao. 2025. Ecotypic divergence in Mongolian Scots pine persists via large-effect genetic adaptation and phenotypic plasticity. *BMC Plant Biol.*, 25: 1642.

Yu, T., Z. Jia, B. Dayananda, J. Li, X. Guo, L. Shi, X. Yuan and Y. Gao. 2022. Analysis of the chloroplast genomes of four *Pinus* species in Northeast China: Insights into hybrid speciation and identification of DNA molecular markers. *J. For. Res.*, 33: 1881-1890.

Zhang, J., G. Lin, Q. Zhao and D.H. Zeng. 2022. High adaptability of *Pinus sylvestris* var. *mongolica* to drought-induced soil nutrient deficiency. *Ecol. Process*, 11: 39.

Zheng, W.J. and L.G. Fu. 1978. Flora Reipublicae Popularis Sinicae (Volume 7). Beijing: Science Press. 203-281.